CrossMark

ORIGINAL ARTICLE

Monte Carlo simulation-aided analytical hierarchy process (AHP) for flood susceptibility mapping in Gabes Basin (southeastern Tunisia)

Noura Dahri[1] · Habib Abida[1]

Abstract Flash floods are among the most severe hazards which have disastrous environmental, human, and economic impacts. This study is interested in the characterization of flood hazard in Gabes Catchment (southeastern Tunisia), considered as an important step for flood management in the region. Analytical hierarchy process (AHP) and geographic information system are applied to delineate and characterize flood areas. A spatial database was developed based on geological map, digital elevation model, land use, and rainfall data in order to evaluate the different factors susceptible to affect flood analysis. However, the uncertainties that are associated with AHP techniques may significantly impact the results. Flood susceptibility is analyzed as a function of weights using Monte Carlo (MC) simulation and Global sensitivity analysis. AHP and MC–AHP models gave similar results. However, compared to AHP approach, MC–AHP confidence intervals (95%) of the overall scores had small overlaps. Results obtained were validated by remote sensing data for the zones that showed very high flood hazard during the extreme rainfall event of June 2014 that hit the study basin.

Keywords Flood hazard · Analytical hierarchy process · Monte Carlo simulation · Tunisia

✉ Noura Dahri
dahri.noura@gmail.com

Habib Abida
habib.abida@fss.rnu.tn

[1] GEOMODELE Laboratory, Faculty of Sciences, University of Sfax, BP 1171, 3000 Sfax, Tunisia

Introduction

Flood is one of the most frequent, widespread, and disastrous natural hazards in Tunisia (Abida and Ellouze 2008). Flash floods happen very suddenly and are difficult to forecast. Flood events generally cause damage to agricultural crops and property, roads and railways, and may even result in the loss of human lives. Millán (2014) affirmed that flash flood hazard is mainly related to the size of the concerned catchment and its geomorphologic characteristics. According to Taubenbock et al. (2011), meteorological conditions and urbanization rates are arguably the most significant driving forces of flood hazard. In arid areas, floods are generally caused by storms of high intensity and are often of relatively limited extent. In these areas, the type of slope and the nature of soil may enhance the potential of rapid surface runoff during intense rainfall. The activation of surface runoff can also be increased by land use modification, urbanization, and fire-induced alteration. Moreover, the dynamics of the socio-economic system and the expansion of urban areas, especially in flood-prone areas, may significantly contribute to raise the damages from flooding events (Elmer et al. 2012).

Gabes Catchment, located in Southern Tunisia on the Mediterranean Sea, is confronted to the impacts entrained by flash floods. The basin is characterized by sparse vegetation, steep slopes, poor soil development, large impermeable areas, high urbanization, and an ever growing population. Besides, rainfall in the region is characterized by its erratic distribution, ranging from extended drought periods to extreme rainfall events resulting in flash floods. In the past, Gabes Region was hit by many flash floods, the most significant of which is the flood of 1962, which resulted in 50 deaths, 7000 persons without shelter and important material losses (Fehri 2014). In the main

🙂 Springer

meteorological station of Gabes City, the analysis of daily precipitation data from September 1983 to December 2014 revealed that intense events represent approximately 23% of the total number of rainy days. The 'extreme' and 'very extreme' events, estimated by percentile indices, correspond to 49.5 and 60.8 mm, respectively. Lately, an extreme rainfall event hit the Gabes Region in June 2014, causing human deaths and major material losses. This resulted in the stagnation of storm water in the numerous low zones of the study area, endangering thereby human health and causing disastrous environmental impacts.

Various methods, used to assess flood susceptibility, are available in the literature. In the context of lacking knowledge about flood phenomena, expertise is required to provide analyses for decision and hazard management purposes using multi-disciplinary qualitative and quantitative approaches. The former is based on expert knowledge to afford a relative indication of hazard while the latter offers quantitative results, based on calculated data and/or modeling. However, these approaches are complementary. Enormous progress has been made in the development of susceptibility mapping and hazard zoning, whereby much of this progress is based on the extensive use of geographic information system (GIS), survey data and remote sensing techniques (Kachouri et al. 2014). GIS environment presents effective tools for handling, integrating, and visualizing diverse spatial data sets (Dixon 2005). The extension of hazard areas is an important consideration in the prediction of flood hazard and the management of natural resources.

One of the most important tools used in hazard mapping is the combination of an analytical hierarchy process (AHP) method (Saaty 1980) with a GIS platform. This process has received significant consideration among multi-disciplinary decision makers and has demonstrated its value in various studies related to natural hazard evaluation, including soil erosion hazard mapping (Kachouri et al. 2014), flood hazard (Fernandez and Lutz 2010), and landslide susceptibility mapping (Feizizadeh et al. 2013). The AHP represents a powerful tool for the analysis of complex decision problems based on an approach of multi-criteria evaluation, generally involving incommensurable data or factors. The integration of AHP into a GIS environment was shown to be efficient in the development of automated methods for quantifying the spatial variability of flood hazard and the associated problems (Pourghasemi et al. 2012).

The application of AHP method has obtained considerable attention and value in various studies related to natural hazard assessment (Dambatta et al. 2009). However, the uncertainties that are associated with AHP techniques may significantly impact the results. The uncertainties are mainly due to incomplete and inaccurate data which are combined into flooded susceptibility values and parameters used in the combination rules. A strong correlation is presented between data uncertainty and parameters uncertainty, since model parameters are obtained directly from measured data, or indirect calibration (Ascough et al. 2008). The large number of parameters and the heterogeneity of data sources make the uncertainty of results difficult to quantify. Thus, AHP technique should be exhaustively evaluated to ensure its robustness under a wide range of possible conditions. The incorporation of probabilistic uncertainty into the AHP technique is considered to quantify the sensitivity and uncertainty of the proposed model. The beta-PERT distribution has been widely used for modeling expert's judgments and providing a close fit to normal distributions with little demand for data (Coates and Rahimifard 2009; Lake et al. 2010). This technique uses the most likely, minimum, and maximum values of expert estimates to generate a probability distribution that provides a possibility of measuring the level of confidence in AHP decision (Chen et al. 2011).

The objective of this study is to examine the magnitude and the extent of flood hazard in Gabes Basin using GIS and AHP techniques. However, this latter is based on expert opinions and thus may be subjected to cognitive limitations with uncertainty and subjectivity (Pourghasemi et al. 2012). Therefore, Monte Carlo simulation-aided analytic hierarchy (MC–AHP) is used to quantify the sensitivity and minimize uncertainty of AHP model. This technique has been already applied to landslide susceptibility mapping (LSM), soil erosion hazard, and pollution control (Cao et al. 2016). To the authors' knowledge, the evaluation of flood hazard remained limited to sensitivity analysis and this the first time that the MC-AHP technique is applied to flood susceptibility mapping (Fernandez and Lutz 2010). The results obtained by the MC–AHP approach were validated based on their confrontation with remote sensing data for the extreme rainfall event that hit the region in June 2014.

This paper is organized as follows. The next chapter (2) presents the study area and describes the methods: AHP, MC–AHP and the validation exercise. Our results are reported and discussed in chapter 3. A conclusion closes the paper in chapter 4.

Materials and methods

Study area and data analysis

Gabes Watershed, located in Southern Tunisia on the Mediterranean Sea, covers a drainage area of 95 km^2. It is characterized by mild slopes and altitudes varying from

0.3 m in the northeast to 235 m in the southwest (Fig. 1). This area is subjected to the influences of both warm and humid air masses coming from the desert and the Mediterranean Sea, respectively. Rainfall is characterized by its shortage, irregularity and erratic distribution, leading to dry and intensive rainy periods, with extreme flood events. Average rainfall is approximately 185 mm/year. Average monthly temperatures vary from 12 °C in January to 29 °C in August, with an annual average of 21 °C. This area is influenced by occasionally strong winds of variable directions. The downstream part of the basin is characterized by its development in terms of housing, industrial, and agricultural activities. Both natural and anthropogenic factors contributed to the damages and impacts of floods.

Six evaluation factors were considered in order to develop a flood susceptibility map of the area (Fernandez and Lutz 2010; Wang et al. 2011; Elsheikh et al. 2015; Dahri et al. 2016; Danumah et al. 2016). They include litho-facies, slope gradient, land use, elevation, rainfall, and drainage density. The analysis starts with the digital elevation model (DEM), created from both real elevation

data and SRTM 30 m data. Real elevation data were derived from the urban management plan. The obtained elevation data were organized as grid data, corresponding to the 1:30,000-scale. The determination of the absolute accuracy of SRTM data is based on the computation of the standard deviation statistic for the elevation differences between the SRTM data and a reference dataset (GPS point measurements) (Gorokhovich and Voustianiouk 2006). The performance of SRTM data involved firstly the conversion of SRTM raster data set into xyz data and then the comparison with observed data in the same location. The results obtained show that a mean difference in elevation between the two data sets is 1.1 m for 110 point measurements. The coefficient of correlation between the two data sets was 0.95. These results indicate a strong positive correlation between the two data sets. Further analysis of the SRTM surface involved a comparison between contours generated from SRTM and the contour maps at a 1:25,000-scale published by the Office of Topography and Cartography (OTC), Tunisia. The results obtained show a reasonably good superposition of the two
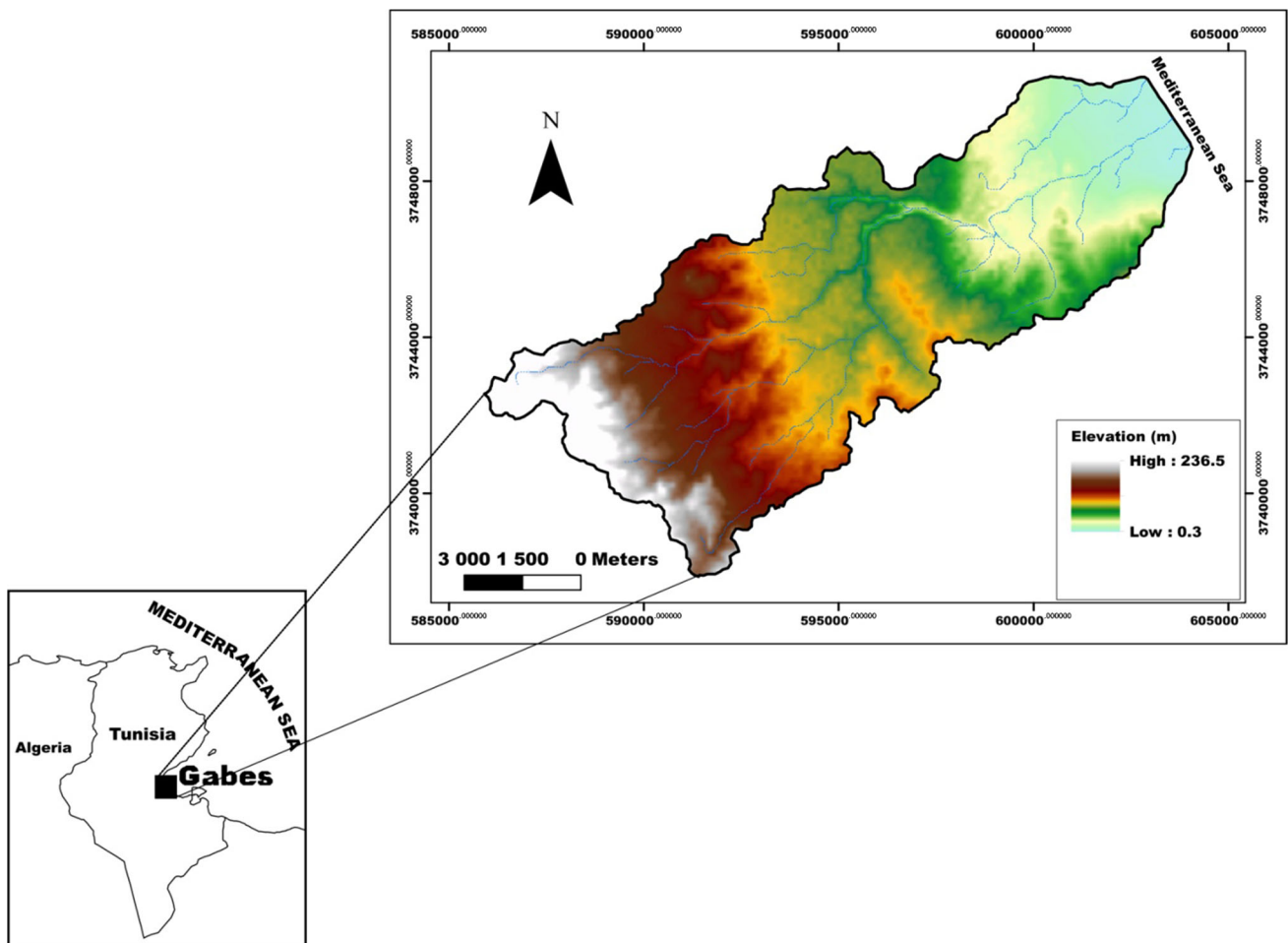

Fig. 1 Location map and digital elevation model of Gabes Catchment

contours derived from the two disparate sources. Further, the superposition of stream networks generated from the two different origins revealed that the two surfaces are generally close. The obtained DEM was adopted to obtain digital thematic layers. Digital slope and stream network layers were also determined on the basis of DEM data. D8 flow direction is the method used to determine the flow direction for each cell according to the steepest descent to one of its 8 neighboring cells (O'Callaghan and Mark 1984). The flow accumulation raster is used for stream delineation. The threshold value for stream network identification depends mostly on climate, basin physical characteristics as well as the spatial resolution of DEM used (Yamamoto 2009). In this study, 1% of the maximum flow accumulation is considered as the default stream threshold value (Girish et al. 2013), computed to be 1055 for Gabes Watershed. This would imply that all cells with flow accumulation value above the threshold are considered to be part of the stream network. A drainage density map was produced from stream network data using the Kernel Density Algorithm. Drainage density is expressed as the total length of the stream network per unit area. The litho-facies basin map resulted from

digitalization of the geological maps (1:50,000) as vector files and then rasterized.

Land use data were obtained by classifying Landsat TM 8 images (Mertikas and Zervakis 2001). The images were classified using a maximum likelihood classification algorithm in a per-pixel classification approach (Sharma et al. 2013). The image classification was run using an appropriate signature file (Fig. 2). Five land use types were identified, including (1) urban area, (2) oasis, (3) forest, (4) low vegetation, and (5) bare soil. This method showed fine details not achieved by photo-interpretation (Mertikas and Zervakis 2001). The overall accuracy and the Kappa coefficient were found to be 93.5% and 0.92, respectively, which clearly shows the accuracy of the classification method (Table 1). The spatial distribution of rainfall data is used to characterize the climatic factor. The thematic layer of rainfall spatial distribution was produced using kriging interpolation (Krige 1951) of data gathered by 6 meteorological stations to create a continuous raster rainfall data within the catchment and its surroundings.

According to Cova (1999), flood hazard assessment is based on the highest rainfall situation. Indeed, extreme
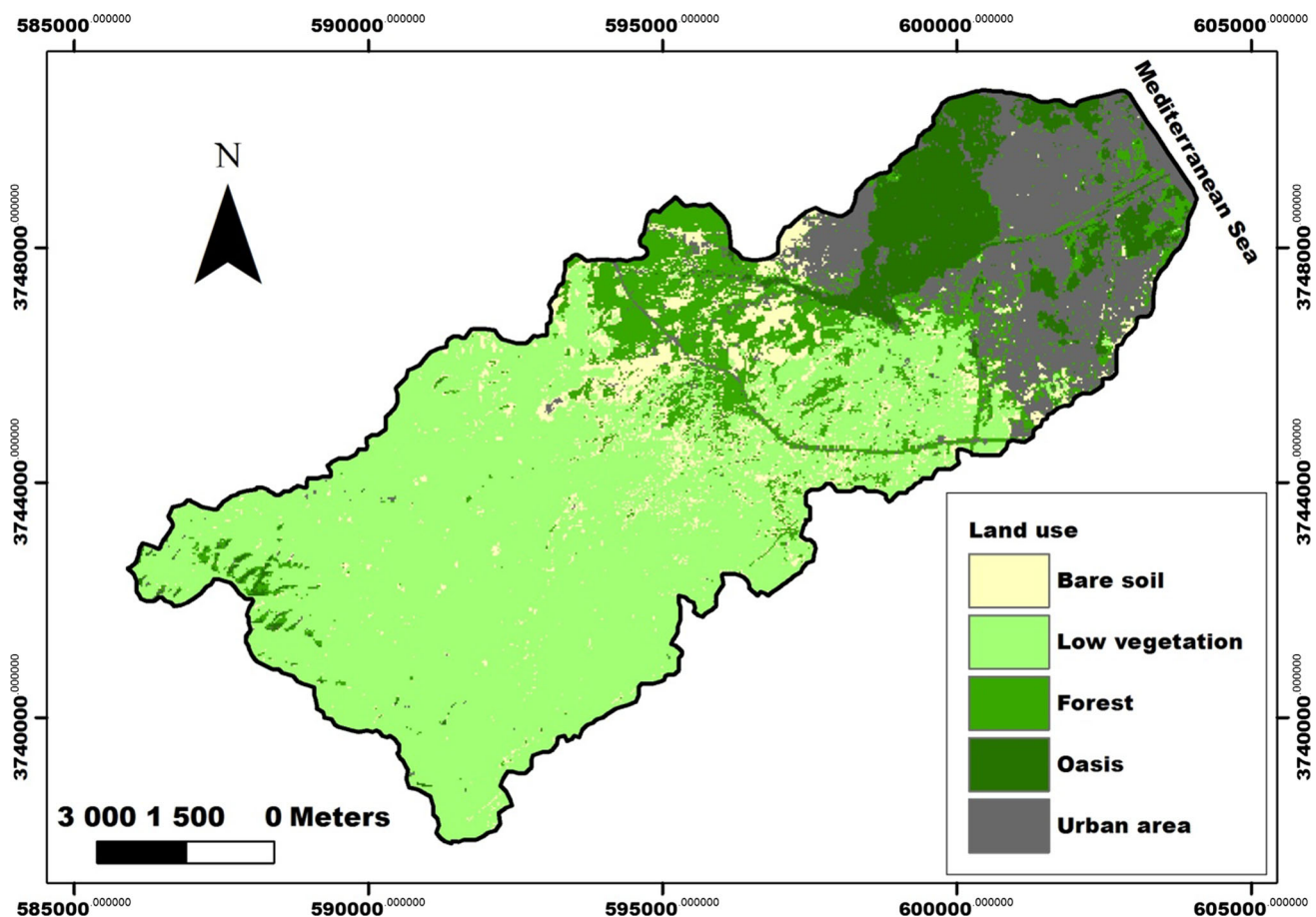

Fig. 2 Land use of Gabes Catchment

Table 1 Kappa statistic and confusion matrix

Overall accuracy = 93.5%

Kappa coefficient = 0.92

Class name	Urban area	Oasis	Low vegetation	Forest	Bare soil
Ground truth (Percent)					
Unclassified	0.16	0.17	0	0	0
Urban area	87.29	2.45	1.24	0	0
Oasis	1.32	95.59	2.35	0	0
Low vegetation	2.48	1.63	88.95	1.71	0.56
Forest	5.45	0	3.87	98.29	0
Bare soil	3.3	0.16	3.59	0	99.44
Total	100	100	100	100	100

Table 2 Statistics of extreme daily rainfall (mm) using Gumbel statistical distribution

T (years)	Gabes_Meteo: 1983–2014		
	Theoretical value	Lower limit	Upper limit
2	36.3	31.87	40.73
5	60	52.54	67.4
10	75.7	65.6	85.8
20	90.8	78.3	103.3
50	110	93.7	126.3
100	125	106.1	143.9
200	140	118.4	161.6
1000	173	145.1	200.9

events are generally used in flood mapping. Rainfall factor in this study was derived from the 2014 extreme event. The maximum registered rainfall over a period of almost 6 h varied between 65 and 110 mm all over Gabes Catchment, showing an erratic spatial rainfall distribution. Downtown Gabes, located downstream, is the area that acquired the maximum of precipitation (from 107 to 110 mm). Gumbel distribution was applied to estimate the recurrence of the annual maximum rainfall recorded during 1 day ($R \times 1d$) over the period extending from 1983 to 2014 (Gumbel 1958; Fehri and Yadh 2016). Table 2 shows that the 2014 extreme rainfall is characterized by a 50 year return period. This is in agreement with the findings of Bourges (1974) who reported that the majority of extreme rainfall events that caused severe damage and human losses in Gabes Region have a return period of 50 years. Finally, all data were projected using the Universal Transverse Mercator (UTM) projection system and arranged as raster maps with a resolution of 20 m for further analysis.

Standardization

Standardization technique is used to translate various inputs of a decision problem to a common scale, to allow comparison, and to overcome the incommensurability of data (Azizur Rahman et al. 2012; Eastman 1997). The standardization process consists in the transformation of the input raster cell values into the [0, 1] range. In this study, the fuzzy module is applied to translate all factors to a common scale [0, 1]. A fuzzy set is an important part of fuzzy logic model (Bellman and Zadeh 1970; Zadeh 1983). The fuzzy sets design is defined by membership functions and rule bases. The membership is the approach that defines the shapes of the fuzzy sets. Fuzzy logic defines the interval between 0 and 1 in order to indicate the various states of truth (Zadeh 1988). This process facilitates the combination of various raster layers regardless of their original measurement scales (Gorsevski et al. 2012). The fuzzy function is selected in such a way that highly suitable raster cells, in terms of achieving the analysis objective, reach high standardized values and less suitable cells are associated with low values (Azizur Rahman et al. 2012).

Analytical hierarchy process (AHP)

Factor weights are assigned to each criterion based on its importance relative to each of the other factors using Saaty's Method (Saaty 1980). AHP is applied to help decision makers make pair-wise comparisons between the factors (Table 3), through an importance scale varying from 1 to 9. The method is weighed for each criterion (W_i) by taking the eigenvector corresponding to the largest eigenvalue of the matrix, and then normalizing the sum of the components to unity (Eq. 1).

$$\sum_{i=1}^{n} W_i = 1 \tag{1}$$

Table 3 Scales for pair-wise AHP comparisons (Saaty and Vargas 1991)

Intensity of importance	Description
1	Equal importance
3	Moderate importance
5	Strong or essential importance
7	Very strong or demonstrated importance
9	Extreme importance
2, 4, 6, 8	Intermediate values
Reciprocals	Values for inverse comparison

The creation of AHP model is based on the following steps:

Step 1: Define the problem and structure its hierarchy which includes a main goal, factors and alternatives.

Step 2: Construct the original basic data which is the pair-wise comparison matrix, PCM, of n factors, established on the basis of Saaty's scaling ratios as defined in Eq. 2. PCM is a matrix with elements a_{ij}. The matrix has also the property of reciprocity (Eq. 3). The construction of pair-wise comparison matrix (PCMs) is based on the surveys and interviews of experts' opinions (eight experts).

$$\text{PCM} = [a_{ij}], i, j = 1, 2, 3 \ldots n \tag{2}$$

$$a_{ij} = 1/a_{ji} \tag{3}$$

Step 3: Use the pair-wise comparison matrix obtained by experts' opinions for each non-diagonal element to generate a corresponding beta distribution (Fazar 1959). Three inputs data (i.e., minimum, maximum, and most likely) are used to fit a beta-PERT distribution. This approach makes the modeling of expert opinions in decision making processes an ideal technique. The PERT formula estimates the average values (mean) and standard deviations (stdev) of non-diagonal elements as defined in Eqs. 4 and 5. These parameters are necessary to calculate shape factors (α and β) from the corresponding beta-PERT distributions (Eqs. 6 and 7).

$$\text{mean} = \frac{\min + 4\,\text{modal} + \max}{p} \tag{4}$$

$$\text{stdev} = \frac{\max - \min}{p} \tag{5}$$

$$\alpha = \left(\frac{\text{mean} - \min}{\max - \min}\right) \cdot \left(\frac{(\text{mean} - \min).(\max - \text{mean})}{\text{stdev}^2} - 1\right) \tag{6}$$

$$\beta = \left(\frac{\max - \text{mean}}{\text{mean} - \min}\right).\alpha \tag{7}$$

Step 4: Stochastically produce the beta-PERT distributions and generate the elements of matrix as defined in Eq. 8.

$$a_{ij} = \min + \text{beta}(\alpha, \beta).(\max - \min) \tag{8}$$

Step 5: Normalize the matrix obtained in step 4. The normalized elements are named b_{ij} which formed a new matrix M_n. The normalization step is defined as shown in Eq. 9

$$b_{ij} = a_{ij} / \sum_{i=1}^{n} a_{ij} \tag{9}$$

Factor's weights are calculated as presented in Eq. 10. The results of Factor's weights are presented in Table 4.

$$W_i = \frac{\sum_{j=1}^{n} b_{ij}}{\sum_{i=1}^{n} \sum_{j=1}^{n} b_{ij}}, i, j = 1, 2, 3 \ldots n \tag{10}$$

Equation 11 represents the relationship between the maximum eigenvalue ($\lambda_{\max}$) and its corresponding eigenvector (W) (Chen et al. 2010).

$$M_n W = \lambda_{\max} W \tag{11}$$

Step 6: Compute the consistency ratio (CR), which reflects the degree of consistency of judgements and determines the quality of the comparison (Saaty 1977). The average random consistency index (RI) is provided in Saaty (1980) (Table 4). The consistency index (CI) results from Eq. 12. CR index is calculated using Eq. 13. CR varies from 0 to 1. A CR value exceeding 0.1 is a sign of inconsistency, and a revision of the preference matrix is recommended. A CR of the order of 0.10 or less represents a reasonable level of consistency.

$$\text{CI} = \frac{(\lambda_{\max} - n)}{n - 1} \tag{12}$$

$$\text{CR} = \frac{\text{CI}}{\text{RI}} \tag{13}$$

Monte Carlo AHP (MC–AHP)

To improve the performance of the proposed model, an innovative Monte Carlo simulation-aided analytic hierarchy process (MC–AHP) is used. This is an important approach to quantify the sensitivity and the uncertainty when weights are assigned based on subjective expert opinion, or personal preference (Gomez-Delgado and Tarantola 2006). This approach is related to probability distributions of all non-diagonal elements of the pair-wise comparison matrix (PCM). In this approach, the same steps and constraints of AHP are used with introduction of beta-random (betarnd function). The betarnd is a function in MATLAB that generates beta distributed numbers within the interval of [0, 1] using to shape factors α and β. The Eq. 8 used in AHP method is replaced by Eq. 14.

$$a_{ij} = \min + \text{betarnd}(\alpha, \beta).(\max - \min) \tag{14}$$

Table 4 Random index RI for different n values

n	3	4	5	6	7	8	9	10	11	12	13	14
RI	0.58	0.9	1.12	1.24	1.32	1.41	1.45	1.49	1.51	1.54	1.56	1.57

Table 5 Factors weights from AHP and MC–AHP approaches

Factor	Classes	AHP-weighting	MC-AHP-weighting
Slope (%)	0–2.2	0.1019	0.1161
	2.2–4.8		
	4.8–9.2		
	9.2–16.1		
	16.1–37		
Elevation (m)	0.3–35.4	0.0883	0.0827
	35.5–70.7		
	70.7–106.8		
	106.8–152.2		
	152.2–237.6		
Litho-facies	Very low impermeable materials	0.1841	0.175
	Low impermeable materials		
	Moderate impermeable materials		
	High impermeable materials		
	Very high impermeable materials		
Rainfall (mm)	67.5–74.9	0.1488	0.1711
	74.9–82		
	82–89.9		
	89.9–97.7		
	97.7–110		
Drainage density (km/km^2)	0–0.8	0.147	0.1484
	0.8–1.8		
	1.8–2.8		
	2.8–4.2		
	4.2–7.3		
Land use	Bare soil	0.3298	0.3068
	Low vegetation		
	Forest		
	Oasis		
	Urban area		

The repetition of the same steps (step (4) to step (6)) of AHP, with Eq. 14 instead of Eq. 8, is considered with a number of replications (raying from 100 to 10.000). The relative weights for factors are obtained (Table 5) and plotted as probability density functions rather than as point values (Jing et al. 2013).

Weighted linear combination (WLC)

Weight values derived from AHP and MC–AHP were assigned to layer factors. Weighted linear combination (WLC) is considered as a decision rule to derive composite maps using GIS platform (Malczewski 1999, 2006). WLC is a concept which aggregates maps by applying a standardized score to each class of factors and a weight to the factors themselves. Factor weights are used to determine the hazard condition (R) as defined by Eq. 15.

$$R = \sum W_i \times X_i \tag{15}$$

W_i is the mean weight values of the factor i, and X_i is the potential rating of the factor i.

Validation

Satellite data were analyzed to identify flood-prone areas (Zhang et al. 2002). A Landsat TM 8 image, captured in June 3, 2014, was used to validate the AHP flood hazard delineation for selected sample points. All bands images were orthorectified, georeferenced to the UTM projection 32 and converted to digital numbers (Knight and Kvaran 2004). Atmospheric correction was also performed to obtain the surface reflectance of all raw images (Devadas et al. 2012). The Landsat image was corrected using ENVI software (Knight and Rvaran 2014; Williams 2008; ITT Visual Information Solutions 2009). Inundated areas were

classified based on thresholds of NDWI (Normalized Difference Water Index) and NDVI (Normalized Difference Vegetation Index), considered to be sufficient to accurately map and monitor the presence of water in natural and artificial ponds. This methodology was tested and verified in arid and semiarid regions (Gond et al. 2004).

Results and discussion

Both GIS and AHP techniques are used to identify flood hazard areas. The AHP method is generally used to describe hazard evaluation (Erkut and Moran (1991). However, for large-scale applications, it is important to incorporate stochastic simulations to better reflect real conditions. This takes into account uncertainty in a real application, which shall increase the confidence of a decision maker in the final results. Monte Carlo simulation, known to be particularly useful in stochastic modeling, was considered. MC–AHP method is based on the fact that input variables are presented as statistical distributions that are derived by best fitting the data

collected. Numerous iterations were performed in order to quantify results and identify the optimum solution. In the following, results of both AHP and MC–AHP are compared based on an error quantification analysis. MC–AHP results were validated using the methodology of Gond et al. (2004). Obtained flooded areas were also verified by survey data collected after a particular flood event.

The obtained flood hazard map of the study area (Fig. 3) was subdivided into five classes, ranging from 'very low' to 'very high' hazard. The areas labeled as 'very high hazard' are strongly influenced by the impervious areas in the urban sector. Impermeable litho-facies and high drainage density tend to increase the flood hazard. The map shows that the northeastern part of Gabes Catchment has the highest flood hazard, with a flooded area of 11.9% of the total area (Table 6). 20.5% of the total area is shown to be under a high level of flood hazard. The areas with very low to low flood hazard are generally located in the southwestern part of the study basin and represent 21.7% of the basin. Table 5 shows that 45.9% of the total area is found to be under a moderate flood hazard. The flood hazard influence is increased mainly downstream of the
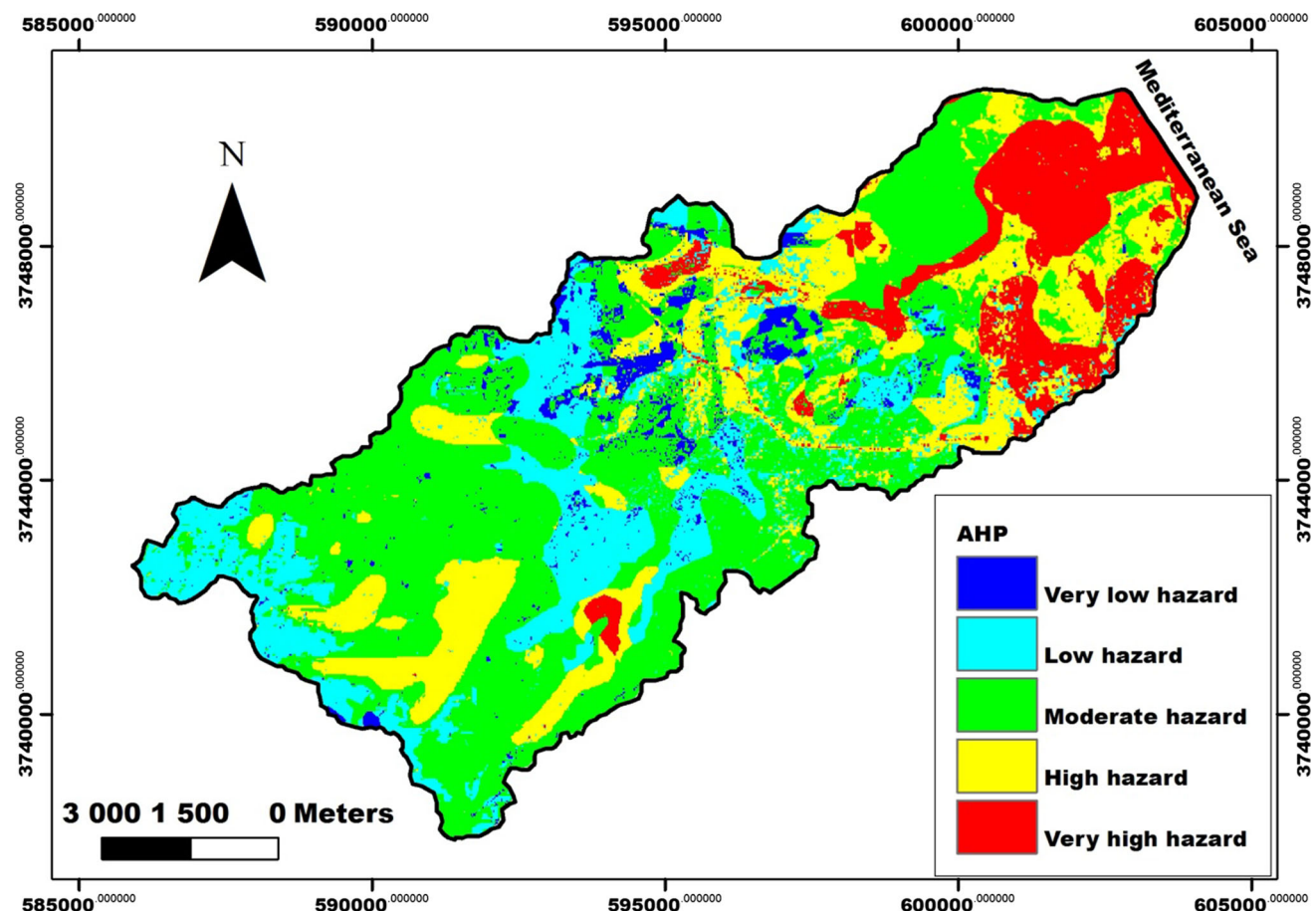

Fig. 3 Final flood susceptibility map derived by AHP approach

Table 6 Subdivision of the different flood risk classes within Gabes Catchment

Classes risk	Area (km^2)	Area (%)
Very high	11.32	11.9
High	19.5	20.5
Moderate	43.6	45.9
Low	17.3	18.2
Very low	3.4	3.5

catchment, characterized by high urbanization rates. Moreover, anarchic urbanization in flood-prone areas and the lack or the limited capacity of the storm water collection system are considered as important factors contributing to flood risk.

The region of 'very high' flood hazard is also located along the coast, which represents the zone that receives the highest amount of rainfall and the most important extreme events. This was demonstrated by Ellouze et al. (2009) who indicated that rainfall increased from the west (continent) to the east (coast line) in southeastern Tunisia regions. Indeed, a high precipitation over a short period of time is the most important factor responsible for triggering floods (Wang et al. 2011). Finally, the urban area located downstream of Gabes Catchment is characterized by mild slopes, inducing thereby water stagnation.

The analytical hierarchy process (AHP), as a method of factors weighting, suffers from sensitivity and uncertainty, as reported by (Banuelas and Antony 2004). The Monte Carlo simulation-aided analytical hierarchy process (MC–AHP) approach is expected to quantify the sensitivity and uncertainty of AHP model. MC–AHP integrated the beta-PERT distribution, which was shown to closely resemble the realistic probability distribution with little demand of data. A PERT normal distribution was considered because the triangular distribution is limited in its ability to model real-world estimates (Jing et al. 2013). The proposed approach addresses the uncertainty resulting from insufficient information and subjectivity judgements in group decision making problems. For all MC–AHP simulations, the consistency ratio was shown to be less than 0.1 (Fig. 4). The results obtained after 10.000 replications show that MC–AHP presented similar results if sorted into five classes (Fig. 5).

The probability density distributions of factor weights obtained by the kernel-smoothing method are plotted in Fig. 6. Compared to other probability density distributions, land use probability function has the most important weights (Fig. 6). Regardless of experts' judgments, the land use factor increased flood hazard especially downstream. The high flood hazard areas are also attributed to mild topography and natural depressions or low points (called Sebkhas) inducing water stagnation. Figure 6 also shows similar flood hazard contributions of both 'rainfall' and 'litho-facies' factors. Finally, elevation contributed with the minimum weight to flood hazard. The results obtained by AHP and MC–AHP were compared. The beta-PERT distribution adopted in the proposed approach significantly reduced standard deviations of the overall scores. Other indices such as confidence interval with a confidence level of 95% were derived for both AHP and MC–AHP as shown in Table 7. In the AHP approach, the overall scores had large variation intervals (Fig. 7). Unlike the traditional AHP method, MC–AHP approach tends to concentrate the weight around the mean with a small confidence interval (Fig. 7). The MC–AHP model mainly reduced

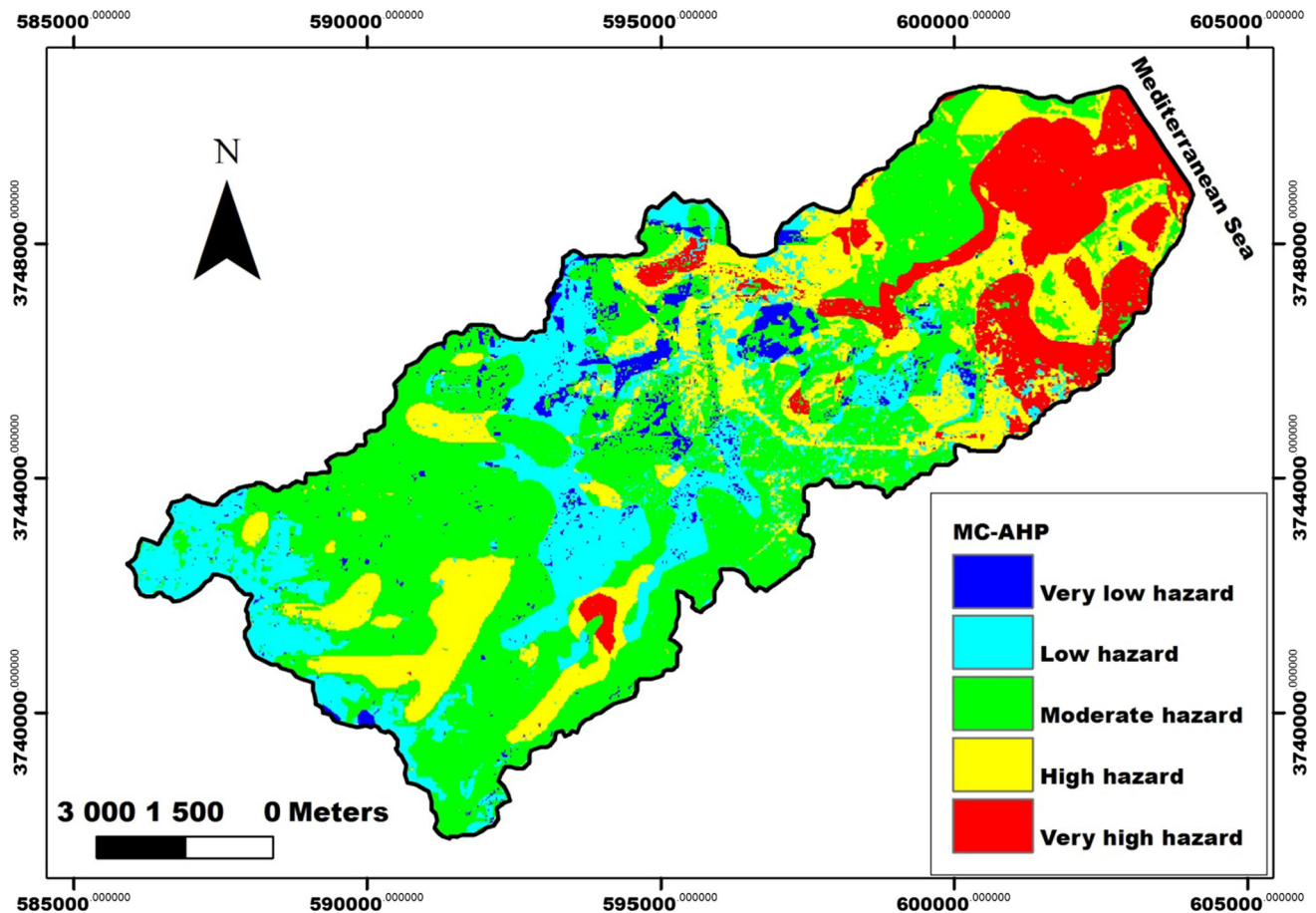**Fig. 4** Consistency ratio of MC–AHP (10.000 Monte Carlo replications)
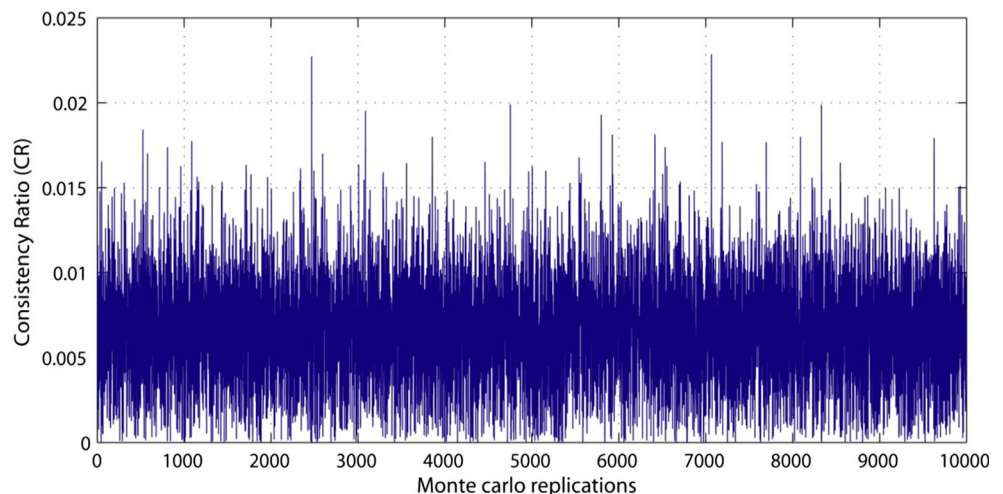
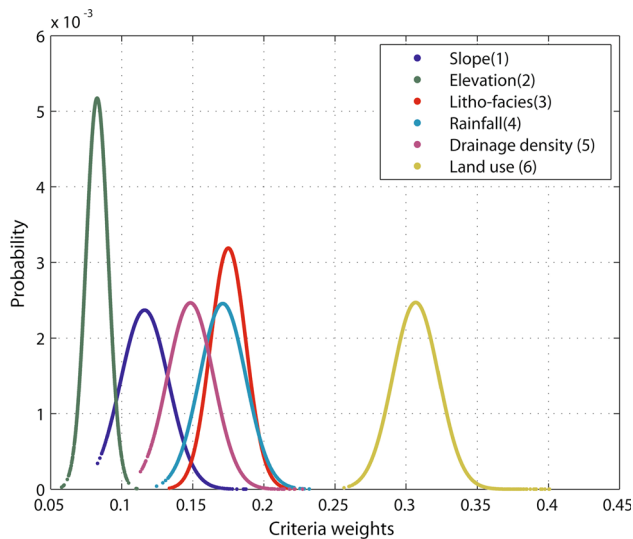Fig. 5 Flood susceptibility map derived by the MC–AHP method

Fig. 6 Probability density estimates of factor weights

the standard deviations of weight factors. This method minimizes the error produced by subjectivity judgments of the AHP model.

The results obtained by the MC–AHP approach were also compared to the Landsat analysis of June 2014 flood event (Fig. 8). The examined flooded areas in 2014 show that 226 observed flood samples are used to validate the accuracy of the results obtained by MC–AHP approach. The total observed inundation area is estimated to be 62 ha (0.65% of total basin area). Two hundred and seven from a total of 226 observed flooding zones are located in a high to very high susceptibility zone. Flood samples are mainly concentrated downstream of the catchment. 95.5% of observed flooding areas are especially located in Gabes City surrounding the streams and anarchic urbanization (Fig. 8). The lack or the limited capacity of the storm water collection system also contributed to water stagnation. Indeed, Gabes City lacks an appropriate drainage system in order to afford a significant level of conveyance, avoiding thereby the multiplication of flooding zones. Storm water is simply conveyed by gravity via roads and streets to the Mediterranean Sea.

Table 7 Statistics for overall scores from the AHP and MC–AHP techniques

| Factors	Mean	Minimum	Maximum	SD	CI
AHP					
Slope	0.1019	0.0411	0.1618	0.0406	(0.022–0.1815)
Elevation	0.0883	0.0352	0.1492	0.0392	(0.0114–0.165)
Litho-facies	0.1841	0.0808	0.261	0.0774	(0.0324–0.336)
Rainfall	0.1488	0.0873	0.2107	0.0586	(0.0339–0.264)
Drainage density	0.147	0.0703	0.1769	0.0387	(0.0711–0.2228)
Land use	0.3298	0.2427	0.4272	0.0728	(0.187–0.4725)
MC-AHP					
Slope	0.1161	0.0266	0.4135	0.0168	(0.1158–0.1164)
Elevation	0.0827	0.0231	0.207	0.0077	(0.0826–0.0828)
Litho-facies	0.175	0.0322	0.3877	0.0125	(0.1747–0.1752)
Rainfall	0.1711	0.053	0.4688	0.0162	(0.1708–0.1713)
Drainage density	0.1484	0.0535	0.4982	0.0162	(0.1481–0.1486)
Land use	0.3068	0.118	0.5991	0.0161	(0.3064–0.3072)
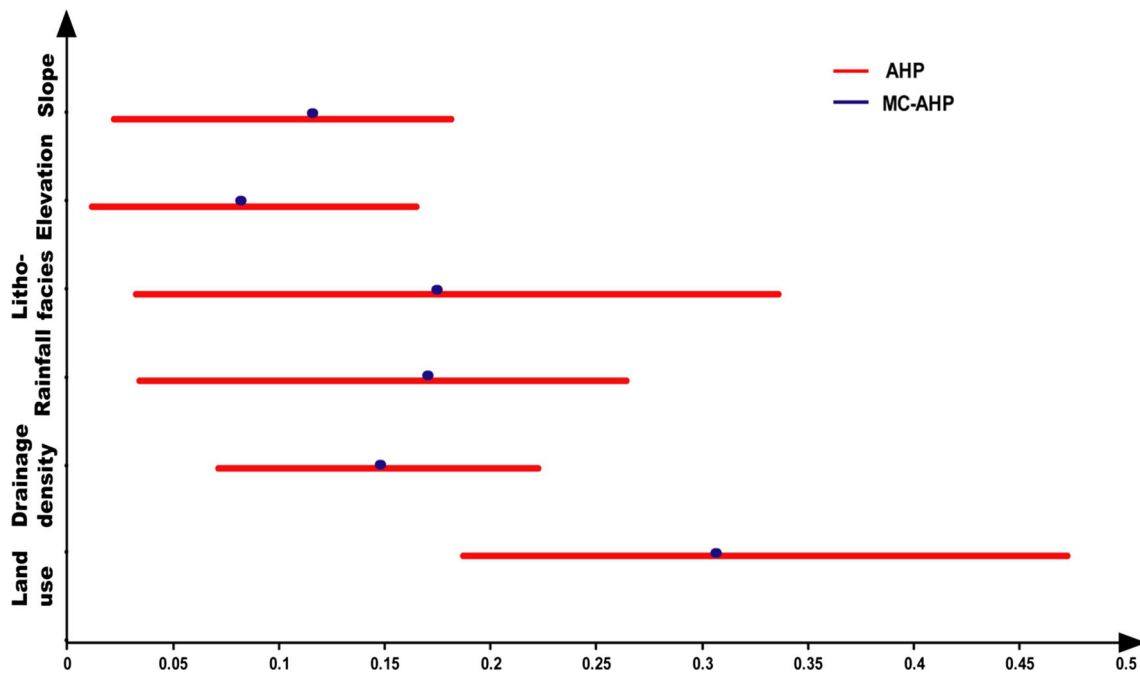
Fig. 7 Confidence interval of 95% plot of the overall scores for the different factors

Conclusion

Analytical hierarchy processes (AHP), with and without Monte Carlo simulation, were applied, and flood susceptibility maps of Gabes Catchment were developed. The analysis considered six variables, including elevation, slope, land use, drainage density, litho-facies, and rainfall. This latter was derived from the spatial distribution of the June 2014 extreme rainfall event, characterized by a return period of 50 years since the concept of hazard is especially associated with extreme events.

The results obtained by both AHP and MC–AHP approaches are similar for five hazard classes. The beta-PERT distribution adopted in the MC–AHP approach significantly reduced standard deviations of overall scores. MC–AHP modified the original factor weights and produced limited confidence intervals. The analysis showed that reducing the error of the input weights results in improving the flood map accuracy. The obtained MC–AHP results show that 33.5% of the basin area is characterized by a high to a very high flooding hazard. Land use was shown to be the most important factor contributing to flood hazard.
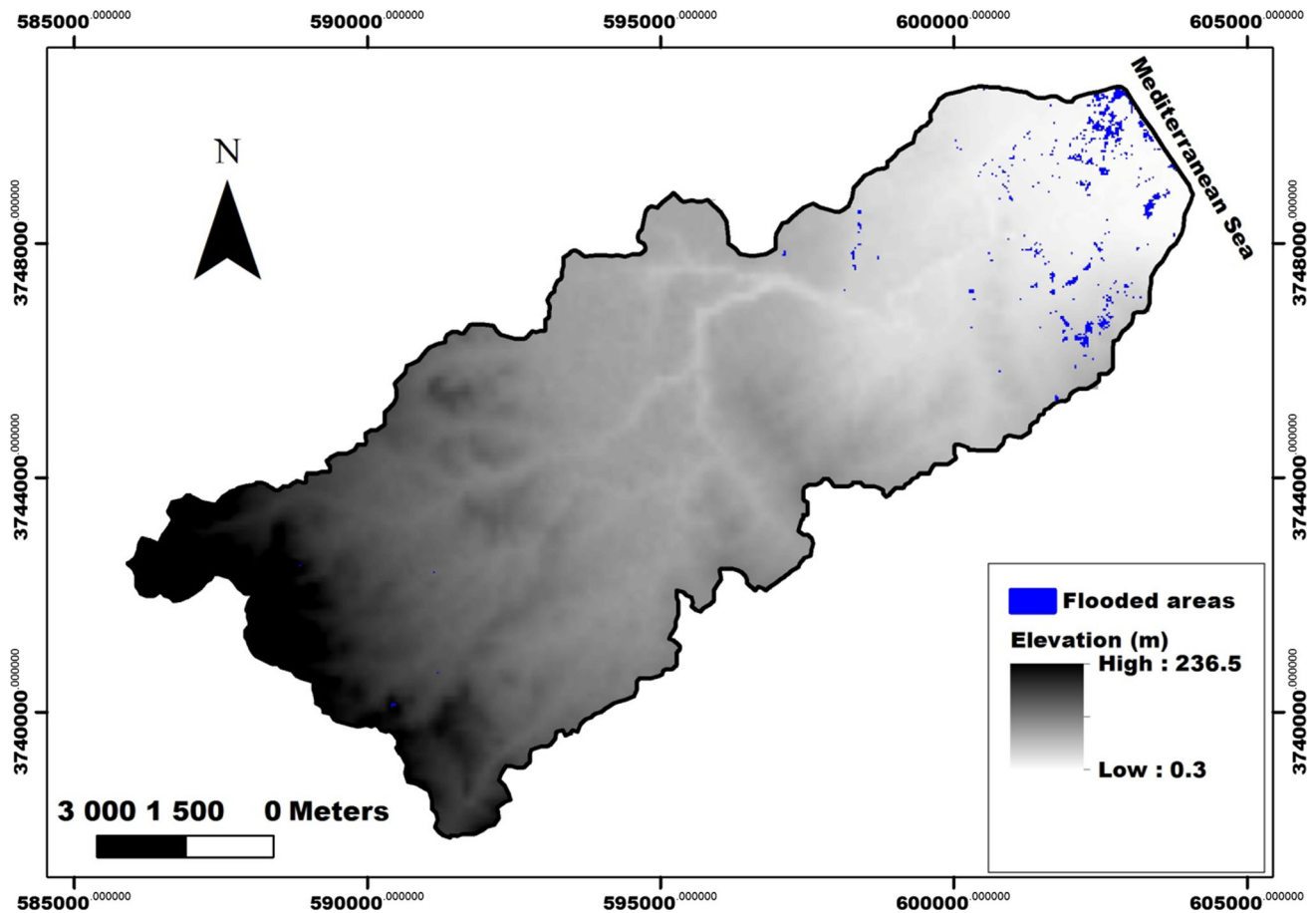
Fig. 8 Land-sat analysis of June 2014 flood event in Gabes Catchment

To validate MC–AHP model, Landsat analysis of the 2014 flood event was used. The examined flooded areas proved that among 226 observed flood samples, 209 zones are characterized by a high to a very high susceptibility hazard. 96.3% of observed flooding areas are located in Gabes City surrounding the streams and anarchic urbanization.

Compliance with ethical standards

Conflict of interest The authors declare no conflict of interest.

References

Abida H, Ellouze M (2008) Probability distribution of flood flows in Tunisia. Hydrol Earth Syst Sci 12:703–714. doi:10.5194/nhess-12-703-2008

Ascough JC, Maier HR, Ravalico JK, Strudley MW (2008) Future research challenges for incorporation of uncertainty in environmental and ecological decision-making. Ecol Model 219:383–399. doi:10.1016/j.ecolmodel.2008.07.015

Banuelas R, Antony J (2004) Modified analytic hierarchy process to incorporate uncertainty and managerial aspects. Int J Prod Res 42:3851–3872

Bellman RE, Zadeh LA (1970) Decision making in a fuzzy environment. Manag Sci 17:141–164

Bourges J (1974) Aperçu sur l'hydrologie du centre sud Tunisien: Réseau d'observations et crues exceptionnelles. O.R.S.T.O.M, Tunisie, pp 1–163

Cao C, Wang Q, Chen J, Ruan Y, Zheng L, Song S, Niu C (2016) Landslide susceptibility mapping in vertical distribution law of precipitation area: case of the Xulong hydropower Station reservoir, Southwestern China. Water 8:270. doi:10.3390/w8070270

Chen Y, Yu J, Khan S (2010) Spatial sensitivity analysis of multi-criteria weights in GIS-based land suitability evaluation. Environ Model Softw 25(12):1582–1591

Chen B, Jing L, Zheng JS, Li P (2011) Integrated management of nonpoint source pollution in the City of Chongzhou, China. In: Technical rep: prepared for the water governance program of United Nations Development Program (UNDP), Beijing, China

Coates G, Rahimifard S (2009) Modelling of post-fragmentation waste stream processing within UK Shredder facilities. Waste Manag 29:44–53. doi:10.1016/j.wasman.2008.03.006

Cova TJ (1999) GIS in emergency management. In: Longley PA, Goodchild MF, Maguire DJ, Rhind DW (eds) Geographical information systems: principles, techniques, applications and management. Wiley, New York, pp 845–858

Dahri N, Ellouze M, Atoui A, Abida H (2016) Mapping flood risk areas in Gabes basin (South-eastern Tunisia). In: International conference on applied geology and environnment 'ICAGE', Tunisia

Dambatta A, Farmani R, Javadi A, Evans B (2009) The analytical hierarchy process for contaminated land management. Adv Eng Inf 23:433–441. doi:10.1016/j.aei.2009.06.006

Danumah JH, Odai SN, Saley BM, Szarzynski J, Thiel M, Kwaku A, Kouame FK, Akpa LY (2016) Flood risk assessment and mapping in Abidjan district using multi-criteria analysis (AHP) model and geoinformation techniques (Cote d'ivoire). Geoenviron Disasters 3:10. doi:10.1186/s40677-016-0044-y

Devadas R, Denham RJ, Pringle M (2012) Support vector machine classification of object-based data for crop mapping, using multi-temporal land sat imagery. Int Arch Photogramm Remote Sens Spat Inf Sci 7:185–190

Dixon B (2005) Applicability of neuro-fuzzy techniques in predicting ground-water vulnerability: a GIS-based sensitivity analysis. J Hydrol 309:17–38

Eastman JR (1997) IDRISI for Windows version 2.0. Tutorial exercises. Worcester-MA, Graduate School of Geography, Clark University, p 192

Ellouze M, Azri C, Abida H (2009) spatial variability of monthly and annual rainfall data over Southern Tunisia. Atmos Res 93:832–839

Elmer F, Hoymann J, Duthmann D, Vorogyshyn S, Kreibich H (2012) Drivers of flood risk change in residential areas. Nat Haz Earth Syst Sci (NHSS) 12:1641-1657. http://www.nat-hazards-earth-syst-sci.net/12/1641/2012/

Elsheikh RFA, Ouerghi S, Elhagi AR (2015) Flood risk map based on GIS and multi criteria techniques (case study Terengganu Malaysia). J Geogr Inf Syst 7:348–357. doi:10.4236/jgis.2015.74027

Erkut and Moran (1991) Locating obnoxious facilities in the public sector: an application of the analytic hierarchy process to municipal landfill siting decisions. Soc Econ Plann Sci 25:89–102

Fazar W (1959) Program evaluation and review technique. Am Stat 13:646–669

Fehri N (2014) L'aggravation du risque d'inondation en Tunis: éléments de réflexion. Physio-Géographie 8:149–175. http://physio-geo.revues.org/3953

Fehri N, Yadh Z (2016) Etude de l'impact de l'extension et de la densification du tissu urbain sur les coefficients de ruissellement dans le bassin   versant des oueds El-Ghrich et   El-Greb (Tunis) par l'application de la méthode SCS aux évènements de septembre 2003. Physio-Géographie 10:61-79. http://physio-geo.revues.org/4685

Feizizadeh B, Blaschke T, Shadman Roodposhti M (2013) Integrating GIS based fuzzy set theory in multicriteria evaluation methods for landslide susceptibility mapping. Int J Geoinf 9:49–57

Fernandez DS, Lutz MA (2010) Urban flood hazard zoning in Tucuman Province, Argentina, using GIS and multicriteria decision analysis. Eng Geol 111:90–98

Girish G, Swtha TV, Ashitha MK (2013) Automated extraction of watershed boundary and drainage network from SRTM and comparison with survey of India topodheet. Arab J Geosci 7:2625–2632

Gomez-Delgado M, Tarantola S (2006) Global sensitivity analysis, gis and multi-criteria evaluation for a sustainable planning of a hazardous waste disposal site in Spain. Int J Geogr Inf Sci 20:449–466

Gond V, Bartholome E, Ouattara F, Nonguierma A, Bado L (2004) Surveillance et cartographie des plans d'eau et des zones humides et inondables en régions arides avec l'instrument vegetation embarqué sur spot-4. Int J Remote Sens 17:987–1004

Gorokhovich Y, Voustianiouk A (2006) Accuracy assessment of the proposed SRTM-based elevation data by CGIAR using field data from USA and Thailand and its relation to the terrain characteristics. Remote Sens Environ 104:409–415

Gorsevski PV, Donevska KR, Mitrovski CD, Frizado JP (2012) Integrating multicriteria evaluation techniques with geographic information systems for landfill site selection: a case study using ordered weighted average. Waste Manag 32:287–296

Gumbel EJ (1958) Statistics of extremes. Columbia University Press, New York

ITT Visual Information Solutions (2009) I.V.I. In atmospheric correction module: quac and flaash user's guide. Version 4.7, ITT Visual Information Solutions: Boulder, CO, USA

Jing L, Chen B, Zhang BY, Li P, Zheng J (2013) Monte Carlo Simulation-aided analytical hierarchy process approach: case study of assessing preferred non-point-source pollution control best management practices. J Environ Eng 139:618–626

Kachouri S, Achour H, Abida H, Bouaziz S (2014) Soil erosion hazard mapping using analytic hierarchy process and logistic regression: a case study of Haffouz watershed, Central Tunisia. Arab J Geosci. doi:10.1007/s12517-014-1464-1

Knight EJ, Kvaran G (2004) Landsat 8 operational land imager design, characterization and performance. Remote Sens 6:10286–10305

Krige DG (1951) A statistical approach to some basic mine valuation problems on the Witwatersrand. J Chem Metall Min Soc S Afr 52:119–139

Lake RJ, Cressey PJ, Campbell DM, Oakley E (2010) Risk ranking for food borne microbial hazards in New Zealand: burden of disease estimates. Risk Anal 30:743–752. doi:10.1111/j.1539-6924.2009.01269.x

Malczewski J (1999) GIS and multicriteria decision analysis. Wiley, Brisbane

Malczewski J (2006) GIS-based multicriteria decision analysis: a survey of the literature. Int J Geogr Inf Sci 20:703–726

Mertikas P, Zervakis ME (2001) Exemplifying the theory of evidence in remote sensing image classification. Int J Remote Sens 6:1081–1095. doi:10.1080/01431160118597

Millán MM (2014) Extreme hydrometeorological events and climate change predictions in Europe. J Hydrol 518:206–224. doi:10.1016/j.jhydrol.2013.12.041

O'Callaghan JF, Mark DM (1984) The extraction of drainage networks from digital elevation data. Comput Vis Graph Image Process 28:328–344

Pourghasemi HR, Pradhan B, Gokceoglu C (2012) Application of fuzzy logic and analytical hierarchy process (AHP) to landslide susceptibility mapping at Haraz watershed, Iran. Nat Hazards 63:965–996

Rahman MA, Rusteberg B, Gogu RC, Lobo Ferreira JP, Sauter M (2012) A new spatial multicriteria decision support tool for site selection for implementation of managed aquifer recharge. J Environ Manag 99:61–75. doi:10.1016/j.jenvman.2012.01.003

Saaty T (1977) A scaling method for priorities in hierarchical structures. J Math Psychol 15:234–281

Saaty T (1980) The analytic hierarchy process. McGraw-Hill International, New York

Saaty TL, Vargas LG (1991) Prediction, projection, and forecasting, applications of the analytic hierarchy process in economics, finance, politics, games, and sports. Kluwer, Boston, p 251

Sharma LK, Nathawat MS, Sinha S (2013) Top-down and bottom-up inventory approach for above ground forest biomass and carbon monitoring in REDD framework using multi-resolution satellite data. Environ Monit Assess 185:8621–8637. doi:10.1007/s10661-013-3199-y

Taubenbock H, Wurm M, Netzband M, Zwenzer H, Rath A, Rahman A, Dech S (2011) Flood risks in urbanized areas—multi-sensoral

approaches using remotely sensed data for risk assessment. Nat Haz Earth Syst Sci (NHSS) 11:431–444. doi:10.5194/nhess-11-431-2011

Wang Y, Li Z, Tang Z, Zeng G (2011) A gis-based spatial multi-criteria approach for flood risk assessment in Dongting lake region, Hunan, Central China. Water Resour Manag 25:3465–3484. doi:10.1007/s11269-011-9866-2

Williams D (2008) Landsat 7 science data users handbook. NASA, Washington

Yamamoto K (2009) How to use ArcHydro. http://www.kristina yamamoto.com/archydro.pdf

Zadeh LA (1983) The role of fuzzy logic in the management of uncertainty in expert systems. Fuzzy Sets Syst 11:199–227

Zadeh LA (1988) Fuzzy logic. Computer 21:83–93

Zhang J, Zhou C, Xu K, Watanabe M (2002) Flood disaster monitoring and evaluation in China. Environ Hazards 4:33–43